Homogeneous Charge Compression Ignition Engine: A Simulation Study on the Effects of Inhomogeneities

P. Maigaard

F. Mauss[1]
e-mail: fabian.mauss@forbrf.lth.se

Division of Combustion Physics,
Lund University,
P. O. Box 118,
22100 Lund, Sweden

M. Kraft
Department of Chemical Engineering,
University of Cambridge,
Cambridge CB2 3RA, UK
e-mail: markus_kraft@cheng.cam.ac.uk

A stochastic model for the HCCI engine is presented. The model is based on the PaSPFR-IEM model and accounts for inhomogeneities in the combustion chamber while including a detailed chemical model for natural gas combustion, consisting of 53 chemical species and 590 elementary chemical reactions. The model is able to take any type of inhomogeneities in the initial gas composition into account, such as inhomogeneities in the temperature field, in the air-fuel ratio or in the concentration of the recirculated exhaust gas. With this model the effect of temperature differences caused by the thermal boundary layer and crevices in the cylinder for a particular engine speed and fuel to air ratio is studied. The boundary layer is divided into a viscous sublayer and a turbulent buffer zone. There are also colder zones due to crevices. All zones are modeled by a characteristic temperature distribution. The simulation results are compared with experiments and a previous numerical study employing a PFR model. In all cases the PaSPFR-IEM model leads to a better agreement between simulations and experiment for temperature and pressure. In addition a sensitivity study on the effect of different intensities of turbulent mixing on the combustion is performed. This study reveals that the ignition delay is a function of turbulent mixing of the hot bulk and the colder boundary layer.
[DOI: 10.1115/1.1563240]

Introduction

The homogeneous charge compression ignition (HCCI) engine is a promising alternative to the existing spark ignition (SI) engines and compression ignition (CI) engines. As in a diesel engine, the fuel is exposed to sufficiently high temperature for autoignition to occur, but for HCCI a homogeneous fuel/air mixture is used. The homogeneous mixture is created in the intake system as in a SI engine, using a low-pressure injection system or by direct injection with very early injection timing. To limit the rate of combustion, very diluted mixtures have to be used. Compared to the diesel engines, the HCCI has a nearly homogeneous charge and virtually no problems with soot and NO_x formation. On the other hand, HC and CO levels are higher than in conventional SI engines. Overall, the HCCI engine shows high efficiency and fewer emissions than conventional internal combustion engines.

The efficiency of the HCCI engine has previously been shown by a number of experiments. Parts of the experiments have been complemented by numerical studies modeling the engine as a plug flow reactor (PFR), [1,2]. In these simulations the ignition delay times for a set of different parameters were investigated. The results indicate that local inhomogeneities are responsible for differences between measurements and simulation results.

One way of accounting for these inhomogeneities is to use multiple zones to model boundary layer effects. Such work has recently been performed using a 10 zone-model for the HCCI engine, [3]. This model is not able to take fluctuations in the zones into account and the chemical source terms are calculated by using the means of temperature and gas composition in the zones. A more sophisticated way is to use a model that is based on the probability density function of the physical variables that are im-

portant in the combustion process. However, the numerical cost, to study chemical reactions together with all aspects of flow in detail, is high and simplifying assumptions have to be introduced. In this paper, we assume that chemical species and temperature are random variables with a probability density function (PDF) that does not spatially vary in the combustion chamber. As in the homogeneous PFR model the combustion chamber is modeled by only one zone, but the gas temperature and composition can fluctuate.

The purpose of this paper is to introduce a new simulation model featuring the partially stirred plug flow reactor (PaSPFR) as described in Refs. [4], [5]. Numerical simulations of the ignition process in the HCCI engine will be performed using a detailed chemical model for butane and lower alkanes in the framework of the PaSPFR. The reaction mechanism contains 53 chemical species and 590 elementary chemical reactions. A simple deterministic IEM model is used to describe the unclosed term for turbulent micromixing in the PaSPFR.

The PaSPFR model, taking fluctuations in temperature that are induced by the colder thermal boundary layer into account, will be used in an attempt to improve on previous numerical simulations of the HCCI process, [1,2]. The results of the new PDF-based model and the old PFR model are compared to experiments in Refs. [1,2]. Additionally, we perform a sensitivity study on the influence of turbulent mixing on ignition delay. The effect of different mixing intensities on the mean of temperature and pressure as well as their standard deviation (STD-DEV) will be discussed.

This discussion is limited to the effect of an assumed initial temperature inhomogeneity. The question how the mixing effects the development of the inhomogeneity will be matter of a later publication.

Previous Model and Experimental Results

The experimental data used in this work are the same as those described in [1]. The experimental setup is as follows: A six-cylinder Volvo TD100 series truck diesel engine has been modi-

Table 1   Volvo TD100 engine parameters

Displaced Volume	1600 cm^3
Bore	120.65 mm
Crank radius	70 mm
Stroke	140 mm
Connection rod	260 mm
Exhaust valve open	39 deg BBDC (at 1 mm lift)
Exhaust valve close	10 deg BTDC (at 1 mm lift)
Inlet valve open	5 deg ATDC (at 1 mm lift)
Inlet valve close	13 deg ABDC (at 1 mm lift)

fied for one-cylinder use, and converted to HCCI operation. The engine data are given in Table 1. The simplest possible combustion chamber geometry is used, i.e., a flat piston crown giving a pancake combustion chamber. Common, commercially available natural gas is used as fuel, [2]. The major compound of the natural gas is methane. The content of higher hydrocarbons such as ethane, propane, and butane (see Table 2 for details) is non-negligible. In Ref. [1] it was demonstrated that the amount of butane in the natural gas is the most sensitive parameter in HCCI combustion with natural gas.

The engine is run on natural gas at fuel-air ratios of $\phi=0.30$–0.45. Four different engine speeds are used: 800, 1000, 1200, and 1400 rpm. These engine speeds are chosen as being representative for normal use considering that maximum torque for a normal CI-operating TD100-series diesel is achieved at 1400 rpm and the engine idle speed is 475–525 rpm. In this work we will focus on the operating conditions stated in Table 3, measured at 60 CAD BTDC.

The detailed reaction mechanism for natural gas that was used in the PFR model predicts the ignition timing correctly. This is shown in Fig. 1. The oscillations in the single cycle curve are due to pressure oscillations. The temperature profile has not been measured but was evaluated from the pressure transducer measurement. The origin of the pressure oscillations is not fully understood. The rate of combustion is most likely so fast that the pressure gradient in the cylinder generates vibrations in the engine structure. These then result in volume changes in the cylinder and hence in pressure oscillations (private communication with B. Johansson).

Modeling the Boundary Layer

As stated above, the assumption of homogeneity is responsible for the rapid temperature rise during ignition or in other words, very short combustion duration. In Ref. [1] it was found that the time of autoignition is mainly dependent on the fuel quality (octane number) and to a lesser extent on initial temperature and fuel/air equivalence ratio.

In Ref. [6] it has been shown that, for the engine under consideration in this paper, inhomogeneities in the fuel charge have only a modest effect on the combustion process. We therefore assume

Table 2   Natural gas components

Component	Mole−%	Mass−%
Methane	91.3	81.0
Ethane	5.0	7.9
Propane	1.8	4.2
n-butane+higher	1.0	4.7
Nitrogen	0.3	0.9
Carbon dioxide	0.6	1.2

Table 3   Initial values for the simulations of engine case (60 CAD BTDC)

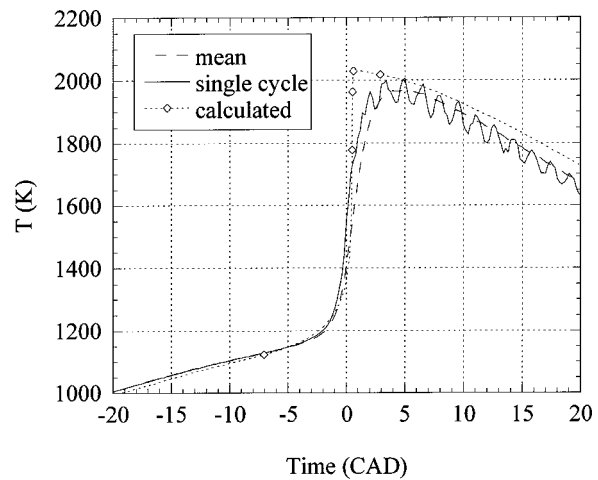| ϕ	CR	T (K)	P (BAR)	RPM
0.368	17.30	664	4.40	1000

Fig. 1   Numerical results from the PFR model compared with experiments. The TD100 engine is in this case run at 1000 rpm and $\phi=0.368$. The jagged line represents results from a single experimental engine cycle and the broken line is its smoothed version.

that the inhomogeneity in the temperature field, caused by the mixing of the colder gases in the boundary layer into the bulk gas, is the most sensitive on the combustion duration. To investigate the influence of the temperature inhomogeneity we model the existence of a colder boundary layer of gas near the cylinder wall at a prescribed crank-angle degree (-60 CAD).

The thickness of this thermal boundary layer has been investigated experimentally on the TD100 series engine, [7]. These experiments suggest that the thickness of the boundary layer is approximately three millimeters. This result coincides with findings from Heywood [8] for the general case. For the current HCCI engine setup a boundary layer of 3 mm corresponds to approximately 15% of the displaced cylinder volume. Since the boundary layer is assumed to be significantly cooler than the bulk gasses, and the average density in the boundary layer is about twice that in the bulk, the total gas mass in the boundary layer will be about 15–20%. Additionally we have to account for colder fluid parcels in crevices.

The boundary layer can be described by applying theories for the flow of a fluid passing a solid surface. It is assumed that it consists of a thin film layer immediately adjacent to the cylinder wall plus a "buffer zone" between this and the turbulent bulk flow, [9]. The crevices are represented by the first five particles and the film layer corresponds to particle numbers 6 to 15 as illustrated in Fig. 2. Within the film layer we have a strong in-
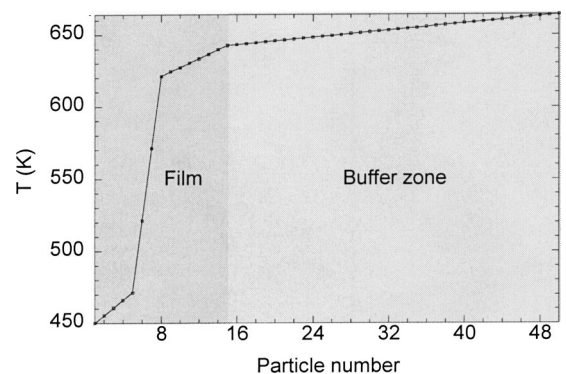

Fig. 2   Temperature distribution in the boundary layer. The temperature increases from the wall temperature and asymptotically approaches the bulk gas temperature.

crease in temperature. This is reflected by the large variance of temperature of the film layer particles. In the viscous sublayer, heat is transferred primarily through conduction.

As one approaches the bulk of the cylinder the temperature increases asymptotically towards the bulk gas temperature (illustrated by the "Buffer zone" in Fig. 2). In Fig. 2 the wall temperature is 450 K and the hot bulk gas is 650 K. The boundary layer is modeled using 50 fluid particles representing the 3 mm radius adjacent to the cylinder wall.

Turbulent Phenomena in the Engine

Experimental results performed on the Volvo TD100 series engine give a quantitative description of the turbulent flow characteristic in the cylinder, [10]. These experiments have been performed under inert or motored conditions and in lean SI mode. In the following we assume that the turbulence characteristics for the engine in HCCI mode are comparable to these results. This assumption is justified by the fact that the same pancake shaped combustion chamber is used in the two setups and that there is no influence on the flow from a propagating flame front in the motored case.

The fluctuating velocity component is defined by the turbulence intensity u' as

$$u' = \lim_{t \to \infty} \left(\frac{1}{t} \int_{t_0}^{t_0+t} u^2 dt \right)^{1/2}$$

and the integral length scale l_I is defined as

$$l_I = \int_0^\infty R_x dx,$$

where R_x is the autocorrelation coefficient of the fluctuating velocity. We assume that the turbulent scalar time scale is related to the fluctuating velocity component by a proportionality constant:

$$\tau_\phi = \frac{\tau}{C_\phi} = \frac{1}{C_\phi} \frac{l_I}{u'},$$

where C_ϕ is a model constant. The turbulent energy dissipation rate ε is given by

$$\varepsilon = \frac{(u')^3}{l_I}.$$

Measurements of turbulence intensity in the cylinder show fluctuations in the range of 0.5–0.9 m/s from 20 CAD BTDC to 20 CAD ATDC. The integral length scale is in the range of 10–18 mm. This gives a turbulence mixing time scale in the order of 0.01 s and a dissipation rate in the order of 10 m²/s³.

The Stochastic Reactor Model

As discussed in the Introduction, we use a stochastic reactor model PaSPFR-IEM from Ref. [4] to describe the influence of inhomogeneities on the combustion process. The assumption of homogeneity for species mass fractions and temperature that has been made previously in [1] is replaced by the assumption of statistical homogeneity. This means that the joint scalar PDF does not vary within the combustion chamber.

In the following, we distinguish between global and local quantities. Global quantities are mass m, volume $V(t)$, mean density $\langle \rho(t) \rangle$, and pressure $p(t)$. We assume that global quantities do not vary spatially in the combustion chamber. Local quantities are chemical species mass fractions $Y_i(t)$, $i = 1, \ldots, S$ and temperature $T(t)$. They can vary within the combustion chamber and are assumed to be random variables. Their joint random vector is defined as

$$\Phi(t) = (\Phi_1, \ldots, \Phi_{S+1}) = (Y_1, \ldots, Y_S, T),$$

and the corresponding joint scalar mass density function (MDF) is given by $F_\Phi(\Psi_1, \ldots, \Psi_{S+1}; t)$ assuming spatial homogeneity as proposed in the PaSPFR model. Its time evolution is given by the following MDF-transport equation:

$$\frac{\partial}{\partial t} F_\Phi(\Psi; t) + \frac{\partial}{\partial \Psi_i} (Q_i(\Psi) F_\Phi(\Psi; t))$$

$$= \frac{\partial}{\partial \Psi_i} \left(\frac{1}{2} \frac{C_\Phi}{\tau} (\Psi_i - \langle \Phi_i \rangle) F_\Phi(\Psi; t) \right),$$

where the initial conditions are given as $F_\Phi(\Psi; 0) = F_0(\Psi)$. The brackets $\langle \cdot \rangle$ denote the mean according to F_ϕ and C_ϕ/τ is a measure for the intensity of scalar mixing. The model constant C_ϕ is set to 2.0, [11] and the turbulent time scale is estimated from the experiment as discussed above. The right-hand side of MDF-transport equation describes the mixing of the scalars by turbulent diffusion. This model is called IEM model and is known to have some deficiencies. It was chosen due to its simplicity and low numerical cost (see details in Ref. [4]). The term Q_i describes the change of the MDF due to chemical reactions, change in volume, and heat losses.

$$Q_i = \frac{M_i}{\rho} \sum_{j=1}^{R} \nu_{i,j} \omega_j \quad i = 1, \ldots, S$$

$$Q_{S+1} = \frac{1}{c_v} \sum_{i=1}^{S} \left(h_i - \frac{RT}{M_i} \right) \frac{M_i}{\rho} \sum_{j=1}^{R} \nu_{i,j} \omega_j + \frac{p}{mc_v} \frac{dV}{dt}$$

$$- \frac{1}{mc_v} (\alpha A (T - T_w) + \sigma \hat{\varepsilon} (T^4 - T_W^4))$$

The convective heat transfer coefficient is obtained from the Woschni equation, [8], σ is the Stefan-Boltzmann constant and the radiation coefficient $\hat{\varepsilon}$ of water and carbon dioxide, [12], is used. Besides the MDF transport equation the time evolution of the global quantities has to be computed. The change of volume $V(\Theta(t))$ in terms of CAD is given by

$$V(\Theta(t)) = V_c + \frac{\pi \cdot B^2}{4} (l + a - a \cdot \cos(l^2 - a^2 \cdot \sin^2 \Theta(t))^{1/2})$$

as in [8]. Mean density can be calculated as

$$\langle \rho(t) \rangle = \frac{m}{V(t)},$$

pressure is given by the ideal gas law

$$p(t) = \langle \rho(t) \rangle \frac{R \langle T \rangle}{\langle M \rangle},$$

where $\langle T \rangle$ is the mean temperature according to the MDF and $\langle M \rangle$ is the expected mean molecular weight. These equations as well as the transport equation of the MDF have to be solved simultaneously. For this work the stochastic reactor model is implemented into the existing code for the calculation of ignition processes in HCCI engines, [1,2], and in the end gas of SI engines as described in [13,14]. The solution procedure is based on a stochastically weighted particle method and a higher-order operator splitting technique. The stochastic particle ensemble approximates the MDF. Each stochastic particle is associated with certain temperature and fluid composition and is thereby related to a fluid particle. Details of the numerical procedure will be published separately.

Initial Conditions

The simulations for the autoignition process were made using initial values obtained from the experiments at 60 CAD BTDC described in Table 3. The species composition in the boundary layer and the bulk is assumed to be homogeneous at 60 CAD
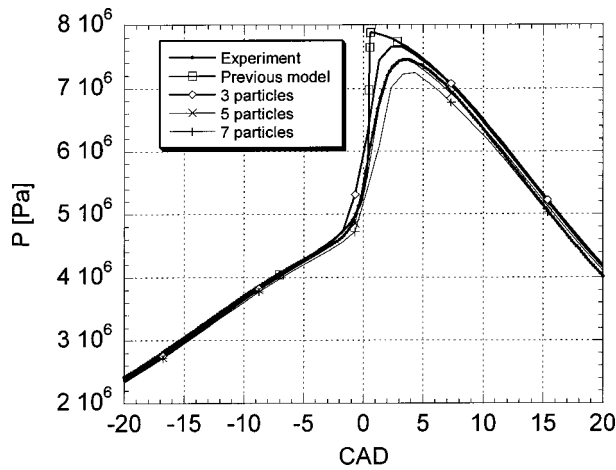
Fig. 3 Pressure history. Results from the new model with varying number of particles are compared to experimental data and a previous model result.
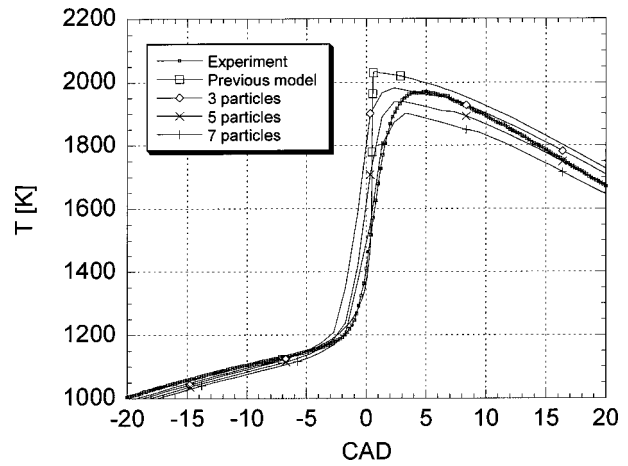

Fig. 4 Temperature history. Results from the new model with varying number of particles are compared to experimental data and a previous model result.

BTDC. During the process inhomogeneities will develop, caused by the inhomogeneous combustion process. The only scalar variable that is assumed to be inhomogeneous at 60 CAD BTDC is the temperature. The initial MDF is given by

$$
F_0(\mathbf{\Psi}) = \underbrace{\sum_{n=1}^{BL} w^{(n)} \delta(\mathbf{\Psi} - \mathbf{\Psi}^{(n)})}_{\text{BoundaryLayer BL}} + \underbrace{w^{(BL+1)} \delta(\mathbf{\Psi} - \mathbf{\Psi}^{(BL+1)})}_{\text{Bulk}}.
$$

The weights $w^{(n)}$ are chosen to be

$$
w^{(n)} = \begin{cases} \dfrac{m_{BL}}{BL} : n = 1, \ldots, BL \\ m_{Bulk} : n = BL + 1 \end{cases}
$$

with $m = m_{BL} + m_{bulk}$ being the mass of the fuel-air mixture in the combustion chamber. The scalars $\Psi_j^{(n)}$ for $j = 1, \ldots, S$ are the chemical species mass fractions and are all set to the same value to meet the conditions in Table 3. The temperature in the boundary layer (BL) $\Psi_{S+1}^{(n)} : n = 1, \ldots, BL$ is set according to the temperature profile displayed in Fig. 2. The temperature in the bulk $\Psi_{S+1}^{(n)} : n = BL + 1$ is set to a value to match the initial mean temperature in the combustion chamber. For the present case we model the boundary layer by choosing a turbulent mixing time scale (τ) of 0.02s and 20% of the total gas mass in the boundary layer.

Results and Discussion

In the following section we demonstrate the capabilities of the new model and compare numerical results with experimental data and results from the previous homogeneous model described in [1]. In the reference case described in Table 3 the engine is operating at 1000 rpm with a fuel/air equivalence ratio of 0.368.

Figure 3 illustrates the pressure history for the reference case. The number of fluid particles representing the viscous sublayer of the film layer and the crevices is varied from three to seven. The shape of the ignition curve is independent of the number of cold particles in this part of the film layer but ignition timing and maximum pressure is affected. Choosing five fluid particles gives a simulated result nearly identical to the experimental results. The new model generally produces results significantly closer to the experiments than the previous model.

Figure 4 shows the temperature history for the same case. The experimental temperature history is not directly measured but calculated from the pressure measurements using a very simple one-

zone model. Therefore the simulated temperature is not directly comparable to the experimental results in this figure.

Figure 5 illustrates the standard deviation (STD-DEV) of the calculated temperature for the simulation. Again the number of fluid particles representing the viscous sublayer of the film layer is varied from three to seven. The STD-DEV is slowly decreasing during the first inert part of the compression stroke due to the temperature mixing of fluid parcels in the bulk and in the boundary layer. At around three CAD BTDC the bulk ignites which leads to a rapid increase of STD-DEV. While the ignition process is progressing the STD-DEV decreases until most of the boundary layer has ignited. The difference in STD-DEV between the time before ignition and after ignition indicates that not all parts of the boundary layer are fully burnt.

Generally one can conclude from these first results that the implementation of the SRM greatly improves the numerical simulation of the HCCI process. The IEM mixing model describes mixing adequately if the initial distribution of particles in crevices and boundary layer is sufficiently good. In the following sections five fluid particles are chosen to represent the laminar part of the film layer.

Sensitivity Study

In this section, we study the effects of varying the turbulence time scale (which is related to turbulence intensity) as predicted
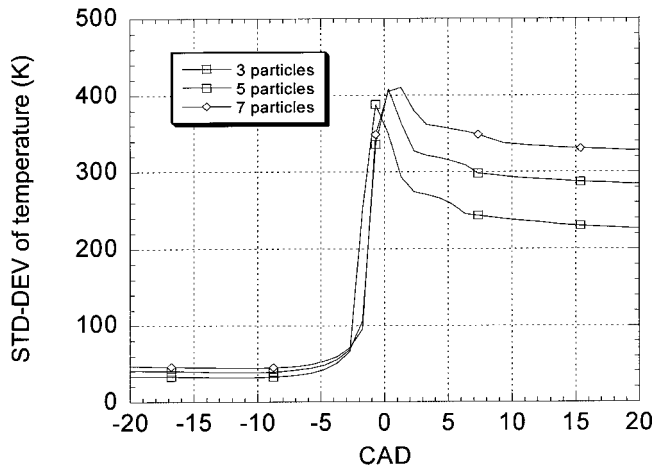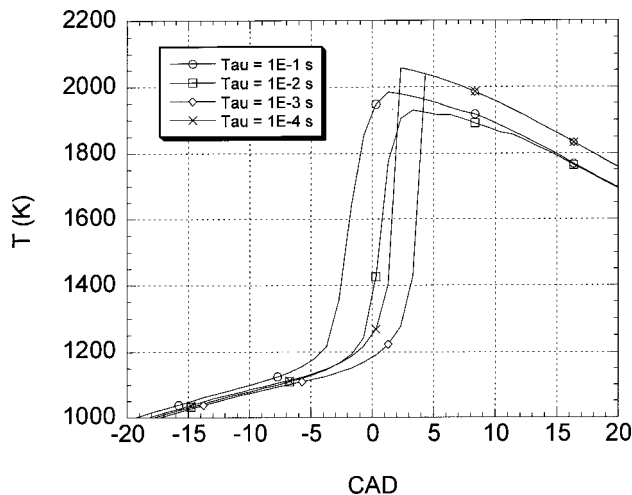

Fig. 5 STD-DEV of temperature history

Fig. 6 Sensitivity study on turbulence mixing time scale (τ)

Fig. 7 STD-DEV of temperature histories for the sensitivity study on turbulence time scale

by the model. It is noted here that we study the influence of the mixing on an existing inhomogeneity. We do not study the development of inhomogeneities caused by the turbulent flow. This means we keep the temperature inhomogeneity at 60 CAD BTDC constant. We further assume that the ongoing cooling of the gas by the wall is not adding inhomogeneity. These assumptions do not hold and a refinement of a stochastic wall–gas interaction model will be matter of a further publication. It is expected that increased turbulent mixing will cause better cooling and thereby will raise the inhomogeneity of the temperature before ignition.

In Fig. 6, the turbulence mixing time scale is varied from 0.1 s to 0.0001 s. The result of this study shows that a very slow mixing ($\tau=0.1$ s) promotes early ignition of the hot spots in the cylinder since they do not mix with the cold spots. As one increases the influence of mixing by decreasing τ the ignition is delayed. At a value of τ of 0.001 s the mixing is now so efficient that a very large region of the fuel and air mixture will ignite simultaneously. At an even smaller value of τ the situation is in essence similar to the homogeneous case and a very steep slope on the ignition curve is observed. These results cannot explain the finding in engines that the combustion duration in engines raises with increasing turbulence in the cylinder, [15]. Again we expect that this finding is caused by the convective cooling of the in cylinder gases, leading to an increased temperature inhomogeneity.

By observing the STD-DEV of temperature for this study in Fig. 7, the mixing effects described above can be better understood. From this graph, it is evident that the bulk ignites earlier in the slow mixing cases as compared to that in fast mixing cases, because of less mixing with the colder boundary layer. As a consequence we find a decrease in the maximum value of the STD-DEV with increasing mixing intensity. As mixing becomes more efficient a time delay between ignition of the colder and hotter spots is noticed.

The effects of mixing in the fast mixing cases are shown in Fig. 8. For $\tau=0.001$ s the mixing is close to perfect before ignition and the STD-DEV is an order of magnitude smaller than for the two slow mixing cases. For $\tau=0.0001$ s the mixing is so fast that no STD-DEV reading is noticeable.

Conclusion

In the present work, a new model for the numerical simulation of the combustion process in the HCCI engine has been presented. This model is based on the PaSPFR-IEM model. It is capable of simulating the influence of inhomogeneities in the cylinder caused by the thermal boundary layer adjacent to the cylinder walls on the combustion process. The model predictions have been compared with engine measurements and numerical results from a
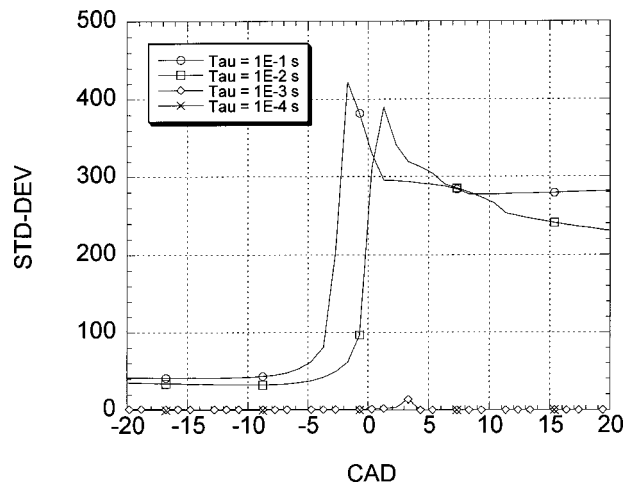
PFR model. Generally the new model shows promising results by significantly improving the quality of the agreement with experimental data compared to the previously used PFR model.

The calculated ignition time histories for temperature and pressure are in very good agreement with the experiments. The modeling of the boundary layer in the cylinder results in a "smoother" ignition curve as the cold and hot spots in the cylinder ignite at different times. In other words, in cylinder temperature inhomogeneities result in an increase of the combustion duration. The STD-DEV of temperature gives evidence that not all of the boundary layer is burnt. This explains the excess of unburnt hydrocarbons from the HCCI engine.

The sensitivity of the turbulent mixing on the combustion process has been investigated. Slow mixing will result in early ignition of the hot spots followed by a delayed ignition of the colder ones. Fast mixing results in almost homogeneous combustion. The weakness of the model is, that it is not able to calculate the origin of the temperature inhomogeneities. It is therefore not able to calculate the influence of different engine geometries on the combustion process.

Future work will discuss the implementation of a more detailed mixing model, e.g., the Curl mixing model. This will increase the demand on CPU time but will give a more accurate description of the mixing processes taking place in the cylinder. A stochastic
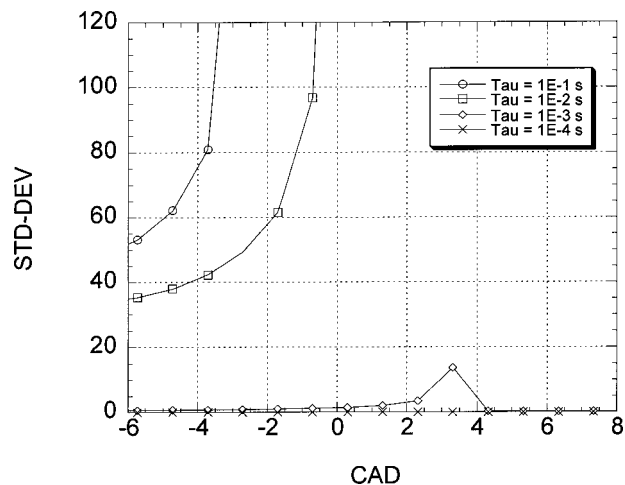

Fig. 8 STD-DEV of temperature. Closeup on the faster mixing cases

wall interaction model needs to be developed to allow the prediction of influence of turbulence intensity on the inhomogeneities in the gases.

Acknowledgments

Nomenclature

Abbreviations

HCCI = homogeneous charged compression ignition
PFR = plug flow reactor
PaSPFR = partially stirred plug flow reactor
PDF = probability density function
MDF = mass density function
IEM = interaction by exchange with the mean mixing model
STD-DEV = standard deviation
ATDC = after top dead center
BTDC = before top dead center
BBTC = before bottom dead center
CAD = crank angle degree
CR = compression ratio
RPM = revolutions per minute
SRM = stochastic reactor model

Arabic Symbols

a = crank radius
A = cylinder surface area
B = bore
c_v = specific heat at constant volume
C_ϕ = proportionality constant
F_ϕ = joint scalar mass density function
h_i = specific enthalpy of species i
l = connecting rod
l_i = integral length scale
m = mass
M = mean molecular weight
M_i = molecular weight of species i
p = pressure
t = time
T = temperature
Q_i = source term
R = universal gas constant
R_x = autocorrelation coefficient
V = volume
V_c = clearance volume
$w^{(n)}$ = mass weight for PDF
Y_i = mass fraction of species i

Greek Symbols

α = heat transfer coefficient
$\hat{\varepsilon}$ = radiation coefficient
ε = dissipation
ϕ = equivalence ratio
$\boldsymbol{\phi}$ = joint scalar random vector
Θ = CAD
ν_{ij} = stoichiometric coefficients
ρ = density
τ = turbulent velocity time scale
τ_ϕ = turbulent scalar time scale
$\boldsymbol{\psi}$ = joint scalar sample variable
ω_j = rate of reaction j

Subscripts and Superscripts

BL = index for boundary layer
Bulk = index for bulk
i = index for scalars
j = index for reactions
n = particle index
S = number of chemical species
R = number of reactions
w = wall

References

[1] Amneus, P., Nilsson, D., Mauss, F., Christensen, M., and Johansson, B., 1998, "HCCI Engine: Experiments and Detailed Kinetic Calculations," *COMODIA 98*, Japan Society of Mechanical Engineers, Tokyo, Japan, pp. 567–572.
[2] Christensen, M., Johansson, B., Amneus, P., and Mauss, F., "Supercharged HCCI Engine," SAE Paper No. 980787.
[3] Aceves, S. M., Flowers, D. L., Westbrook, C. K., Smith, J. R., and Pitz, W., 2000, "A Multi-Zone Model for Prediction of HCCI Combustions and Emissions," SAE Paper No. 2000-01-0327.
[4] Kraft, M., 1998, "Stochastic Modelling of Turbulent Reacting Flow in Chemical Engineering," VDI Verlag, Fortschrittsberichte des VDI, Reihe **6**(391).
[5] Procaccini, C., Kraft, M., Fey, H., Bockhorn, H., Longwell, J. P., Sarofim, A., and Smith, K. A., 1998, "PIC Formation During the Combustion of Simple Hydrocarbons in Inhomogeneous Incineration Systems," Proc. Combust. Inst., **27**, pp. 1275–1281.
[6] Richter, M., Engström, J., Franke, A., Aldén, M., Hultqvist, A., and Johansson, B., 2000, "The Influence of Charge Inhomogeneity on the HCCI Combustion Process," SAE Paper No. 2000-FL-633.
[7] Hultqvist, A., Christensen, M., Johansson, B., Franke, A., Richter, M., and Alden, M., "A Study of the HCCI Combustion Process by Chemiluminescence Imaging," SAE Paper No. 1999-01-3680.
[8] Heywood, J. B., 1989, "*Internal Combustion Engine Fundamentals*," McGraw-Hill, New York.
[9] Perry, R. H., *Perry's Chemical Engineers' Handbook*, 6th Ed., McGraw-Hill, New York.
[10] Johansson, B., 1995, "On Cycle to Cycle Variations in Spark Ignition Engines," Doctoral thesis, Lund Institute of Technology.
[11] Pope, S. B., 1985, "PDF Methods for Turbulent Reactive Flows," Prog. Energy Combust. Sci., **11**, pp. 119–192.
[12] Hottel, H. C., 1954, *Radiant Heat Transmission*, 3rd Ed., W. H. Adams, ed., McGraw-Hill, New York.
[13] Hajireza, S., Mauss, F., and Sundén, B., 1997, "Investigation of End-Gas Temperature and Pressure Increases in Gasoline Engines and Relevance for Knock Occurrence," SAE Paper No. 971671.
[14] Bood, J., Bengtsson, P.-E., Mauss, F., Burgdorf, K., and Denbratt, I., 1997, "Knock in Spark-Ignition Engines: End-Gas Temperature Measurements Using Rotational CARS and Detailed Kinetic Calculations of the Autoignition Process," SAE Paper No. 971669.
[15] Christensen, M., Johansson, B., and Hultquist, A., "The Effect of Combustion Chamber Geometry on HCCI Operation," SAE Paper No. 2002-01-0425.